PM/99–57
December 1999
LC-TH-2000-028

Associated Production of Higgs Bosons with Scalar Quarks at $\mathbf{e^+e^-}$ Linear Colliders

A. Djouadi, J.L. Kneur and G. Moultaka

Laboratoire de Physique Mathématique et Théorique, UMR5825–CNRS,
Université de Montpellier II, F–34095 Montpellier Cedex 5, France.

Abstract

We analyze the production of neutral Higgs particles in association with the supersymmetric scalar partners of top and bottom quarks at future e^+e^- linear machines, including the $\gamma\gamma$ option. In the Minimal Supersymmetric extension of the Standard Model, the cross section for the associated production of the lightest neutral h boson with these squarks can be rather substantial. These processes would open a window for the measurement of the $h\tilde{t}\tilde{t}$ and $h\tilde{b}\tilde{b}$ couplings.

Contribution to the *2nd ECFA–DESY Study on Physics and Detectors for a Linear Electron–Positron Collider*, Orsay–Frascati–Lund–Oxford–Obernai–Padova (1998–2000).

Associated Production of Higgs Bosons with Scalar Quarks at e^+e^- Linear Colliders

A. Djouadi, J.L. Kneur and G. Moultaka

Laboratoire de Physique Mathématique et Théorique, UMR5825–CNRS,
Université de Montpellier II, F–34095 Montpellier Cedex 5, France.

Abstract

We analyze the production of neutral Higgs particles in association with the supersymmetric scalar partners of top and bottom quarks at future e^+e^- linear machines, including the $\gamma\gamma$ option. In the Minimal Supersymmetric extension of the Standard Model, the cross section for the associated production of the lightest neutral h boson with these squarks can be rather substantial. These processes would open a window for the measurement of the $h\tilde{t}\tilde{t}$ and $h\tilde{b}\tilde{b}$ couplings.

1. Introduction

One of the firm predictions of the Minimal Supersymmetric Standard Model (MSSM) [1] is that, among the quintet of scalar [two CP–even h and H, a pseudoscalar A and two charged $H^{\pm}$] particles contained in the extended Higgs sector [2], the lightest Higgs boson h should be rather light, with a mass $M_h \lesssim 130$ GeV [3]. This Higgs particle should therefore be produced at the next generation of high–energy colliders [4, 5], or even before [6, 7], if supersymmetry (at least its minimal version) is indeed realized in Nature. At future high–energy and high–luminosity e^+e^- colliders, with center of mass energies in the range 350–500 GeV, the properties of this particle should be studied in great detail [5], to shed some light on the electroweak symmetry breaking mechanism.

In the MSSM, the genuine SUSY particles, neutralino/charginos and sfermions could have masses not too far from the electroweak symmetry breaking scale. In particular the lightest neutralino, which is expected to be the lightest SUSY particle (LSP), could have a mass in the range of ~ 100 GeV. Another particle which could also be light is one of the spin–zero partners of the top quark, the lightest stop $\tilde{t}_1$. Indeed, because of the large m_t value, the two current stop eigenstates could strongly mix [8], leading to a mass eigenstate $\tilde{t}_1$ much lighter than the other squarks [which are constrained to be rather heavy [9, 10] by the negative searches at the Tevatron] and even lighter than the top quark itself. Similar features can also occur in the sbottom sector. These particles could therefore be also easily accessible at the next generation of e^+e^- colliders.

If the mixing between third generation squarks is large, stops/sbottoms can not only be rather light but at the same time their couplings to Higgs bosons can be strongly enhanced. In particular, the (normalized) $h\tilde{t}_1\tilde{t}_1$ coupling can be the largest electroweak coupling in the MSSM. This might have a rather large impact on the phenomenology of the MSSM Higgs bosons as was stressed in Ref. [11]. The measurement of this important coupling would open a window to probe directly some of the soft–SUSY breaking terms of the potential. To measure Higgs–squarks couplings directly, one needs to consider the three–body associated production of Higgs bosons with scalar quark pairs [12, 13]. This is similar to the processes of Higgs boson radiation from the top quark lines at e^+e^- [14] colliders, which allow to probe the $t\bar{t}$–Higgs Yukawa coupling directly.

In this note, we discuss the production of Higgs particles in association with third generation scalar quarks at future high–energy e^+e^- linear machines, including the $\gamma\gamma$ option. We will illustrate our numerical results in the case of the unconstrained MSSM as well as in the minimal SUGRA case.

2. Physical Set–Up

2.1 Masses and Couplings

In the case of the third generation, the left– and right–handed sfermions $\tilde{q}_L$ and $\tilde{q}_R$ [the current eigenstates] can strongly mix [8]; for a given squark $\tilde{q} = \tilde{t}, \tilde{b}$, the mass matrices which determine the mixing are given by

$$M_{\tilde{q}}^2 = \begin{bmatrix} m_{LL}^2 + m_q^2 & m_q \tilde{A}_q \\ m_q \tilde{A}_q & m_{RR}^2 + m_q^2 \end{bmatrix} \tag{1}$$

with, in terms of the soft SUSY–breaking scalar masses $m_{\tilde{q}_L}$ and $m_{\tilde{q}_R}$, the trilinear squark coupling A_q, the higgsino mass parameter μ and $\tan\beta = v_U/v_D$, the ratio of the vacuum expectation values of the two–Higgs doublet fields:

$$m_{LL}^2 = m_{\tilde{q}_L}^2 + (I_3^q - e_q s_W^2) \cos 2\beta \, M_Z^2 \ , \ m_{RR}^2 = m_{\tilde{q}_R}^2 + e_q s_W^2 \ \cos 2\beta \, M_Z^2$$
$$\tilde{A}_q = A_q - \mu (\tan\beta)^{-2I_3^q} \tag{2}$$

I_3^q and e_q are the weak isospin and electric charge of the squark $\tilde{q}$, and $s_W^2 = 1 - c_W^2 \equiv \sin^2\theta_W$. The mass matrices are diagonalized by 2×2 rotation matrices of angle θ_q. The mixing angles and the squark eigenstate masses are then given by

$$\sin 2\theta_q = \frac{2 m_q \tilde{A}_q}{m_{\tilde{q}_1}^2 - m_{\tilde{q}_2}^2} \quad , \quad \cos 2\theta_q = \frac{m_{LL}^2 - m_{RR}^2}{m_{\tilde{q}_1}^2 - m_{\tilde{q}_2}^2} \tag{3}$$

$$m_{\tilde{q}_{1,2}}^2 = m_q^2 + \frac{1}{2}\left[m_{LL}^2 + m_{RR}^2 \mp \sqrt{(m_{LL}^2 - m_{RR}^2)^2 + 4 m_q^2 \tilde{A}_q^2} \right] \tag{4}$$

Due to the large value of m_t, the mixing is particularly strong in the stop sector, unless $\tilde{A}_t = 0$. This generates a large splitting between the masses of the two stop eigenstates, possibly leading to a lightest top squark much lighter than the other squarks and even lighter than the top quark. For large values of $\tan\beta, \mu$ and/or A_b the mixing in the sbottom sector can also be rather large, leading in this case to a possibly light $\tilde{b}_1$.

In the constrained MSSM or minimal SUGRA [15], the soft SUSY breaking scalar masses, gaugino masses and trilinear couplings are universal at the GUT scale; the left– and right–handed sfermion masses are then given in terms of the gaugino mass parameter

$m_{1/2}$, the universal scalar mass m_0 and $\tan\beta$. For instance in the small $\tan\beta$ regime, the two soft scalar top masses [in which we include also the D–terms] at the low energy scale obtained from the one–loop RG evolution [16], are approximately given by [17]:

$$\begin{aligned} m^2_{\tilde{t}_L} &= 0.51 m_0^2 + 5.29 m_{1/2}^2 + 0.35 M_Z^2 \cos 2\beta \\ m^2_{\tilde{t}_R} &= 0.01 m_0^2 + 3.68 m_{1/2}^2 + 0.15 M_Z^2 \cos 2\beta \end{aligned} \tag{5}$$

This shows that, in contrast with the first two generations, one has generically a sizeable splitting between $m^2_{\tilde{t}_L}$ and $m^2_{\tilde{t}_R}$ at the electroweak scale, due to the running of the (large) top Yukawa coupling [expect possibly in the marginal region where m_0 *and* $m_{1/2}$ both become very small]. Thus degenerate left and right soft stop masses [at the electroweak scale] will be considered only in the unconstrained MSSM. Note that in this case, in most of the MSSM parameter space, the mixing angle eq. (3) is either close to zero [no mixing] or to $-\pi/4$ [maximal mixing] for respectively, small and large values of the off–diagonal entry $m_t \tilde{A}_t$ of the squark mass matrix eq. (1).

The couplings of a neutral MSSM Higgs boson $\Phi = h, H, A$ to a pair of squarks $\tilde{q}_i \tilde{q}_j$ can be found in Ref. [13]. In the decoupling limit, $M_A \sim M_H \gg M_Z$, the mixing angle α which enters the couplings reaches the limit $\beta - \pi/2$, and the expressions of the couplings become rather simple. One would then have for the $h\tilde{t}\tilde{t}$ couplings for instance

$$\begin{aligned} g_{h\tilde{t}_1\tilde{t}_1} &= \cos 2\beta \left[\frac{1}{2}\cos^2\theta_t - \frac{2}{3} s_W^2 \cos 2\theta_t \right] + \frac{m_t^2}{M_Z^2} + \frac{1}{2}\sin 2\theta_t \frac{m_t \tilde{A}_t}{M_Z^2} \\ g_{h\tilde{t}_2\tilde{t}_2} &= \cos 2\beta \left[\frac{1}{2}\sin^2\theta_t - \frac{2}{3} s_W^2 \cos 2\theta_t \right] + \frac{m_t^2}{M_Z^2} - \frac{1}{2}\sin 2\theta_t \frac{m_t \tilde{A}_t}{M_Z^2} \\ g_{h\tilde{t}_1\tilde{t}_2} &= \cos 2\beta \sin 2\theta_t \left[\frac{2}{3} s_W^2 - \frac{1}{4} \right] + \frac{1}{2}\cos 2\theta_t \frac{m_t \tilde{A}_t}{M_Z^2} \end{aligned} \tag{6}$$

involving components that are proportional to $\tilde{A}_t = A_t - \mu/\tan\beta$. For large values of the parameter $\tilde{A}_t$, which incidentally make the $\tilde{t}$ mixing angle almost maximal, $|\sin 2\theta_{\tilde{t}}| \simeq 1$, the last components can strongly enhance the $g_{h\tilde{t}_1\tilde{t}_1}$ coupling and make it larger than the top quark coupling of the h boson, $g_{htt} \propto m_t/M_Z$. The couplings of the heavy H boson to stops involve also components which can be large. The pseudoscalar A boson couples only to $\tilde{t}_1\tilde{t}_2$ pairs because of CP–invariance.

2.2 Constraints used in the numerical analysis

We will illustrate our numerical results in the case of the unconstrained MSSM as well as in the minimal SUGRA case. We will concentrate on the case of the lightest h boson of the MSSM in the decoupling regime [18], and discuss only the production in association with light top squarks [in the case of no mixing, this corresponds to both squarks $\tilde{t}_1, \tilde{t}_2$ since their masses are almost equal, while in the case of large mixing this would correspond to the lightest top squark $\tilde{t}_1$]. That is, we consider the range of the MSSM input parameters in such a way that $M_h \ll M_H \simeq M_A \simeq M_{H^\pm}$, which also implies for the mixing angle α

of the neutral CP–even Higgs sector $\alpha \simeq \beta - \pi/2$. In this approximation, the behavior of the $\tilde{t}\tilde{t}h$ coupling with respect to the SUSY–breaking parameter $\tilde{A}_t$ is very simple, as discussed in the previous subsection.

The approximation of being close to the decoupling limit implies that we do not consider other Higgs production processes [although the analytical expressions [13] will also hold in these cases] with e.g. the heavy neutral H or CP–odd A bosons produced in association with top squarks. In any case, these processes would be suppressed by phase–space well before the decoupling regime is reached [this is even more legitimate in the minimal SUGRA case, where for most of the parameter space allowed by present experimental limits, the MSSM Higgs sector turns out to be in this decoupling regime; see Ref. [19] for instance]. The production of the h boson in association with light sbottoms [that we will also not consider in the numerical analysis] should follow the same pattern as for the stops, except that one has to replace the $\tilde{t}_1\tilde{t}_1h$ coupling by the $\tilde{b}_1\tilde{b}_1h$ coupling; the latter being strongly enhanced for large $\tan\beta$ and μ values.

Note that, in general, we will use as input the parameters soft scalar masses [taken to be qual in general $m_{\tilde{q}_L} = m_{\tilde{q}_R} = m_{\tilde{q}}$], A_t, $\tan\beta$ and μ. The h boson mass is then calculated as a function of these parameters [M_h is only marginally affected by the variation of the parameter μ] with the pseudoscalar Higgs boson mass fixed to $M_A = 1$ TeV, and with the full radiative corrections in the improved effective potential approach [3] included.

Let us now discuss the constraints which will be used in our numerical analysis. First there are of course the experimental bounds on the top squark and Higgs boson masses. From negative searches at LEP2, a bound $m_{\tilde{t}_1} \gtrsim 80$ GeV is set on the lightest top squark mass [9]. Larger masses, up to $m_{\tilde{t}_1} \sim 120$ GeV, are excluded by the CDF collaboration [10] in the case where the lightest neutralino is not too heavy, $m_{\chi_1^0} \lesssim 50$ GeV.

The general experimental lower bound on the lightest h boson in the MSSM from LEP2 negative searches is $M_h \gtrsim 80$ GeV [9]. However, in the decoupling limit the h boson will behave as the SM Higgs particle for which the lower bound is larger, $M_h \gtrsim 90$ GeV; this will be the lower bound which will be used practically in our analysis since we will work mostly in the decoupling regime. This calls for relatively large values of the parameter $\tan\beta$ [since the maximal value of M_h increases with increasing $\tan\beta$] and/or large mixing in the top squark sector [the "maximal mixing" scenario, in which the h boson mass is maximized for a given $\tan\beta$ value, is for $A_t \simeq \sqrt{6}m_{\tilde{q}}$].

Here, we will often focus on the large–A_t/small–$m_{\tilde{t}_1}$ scenario, which gives the largest $\tilde{t}_1\tilde{t}_1h$ production cross sections. However there are theoretical as well as experimental constraints on this scenario which should also be taken into account in the analysis: *i)* The absence of charge and color breaking minima (CCB) [20] can put rather stringent bounds on the parameter $\tilde{A}_t$: for the unconstrained MSSM case, a stringent CCB constraint for a large A_t scenario reads: $A_t^2 < 3(m^2_{\tilde{t}_L} + m^2_{\tilde{t}_R} + \mu^2 + m^2_{\Phi_U})$. *ii)* Large values of $\tilde{A}_t$ lead to a large splitting of the top squark masses; this breaks the custodial SU(2) symmetry, generating potentially large contributions to electroweak high–precision observables, and in particular to the ρ parameter, whose leading contributions are proportional to different combinations of the squared squark masses, and which is severely constrained by LEP1 data [21]. Since this is potentially the most restrictive constraint on a large A_t scenario, we have thus evaluated precisely the contributions of the $(\tilde{t}, \tilde{b})$ isodoublet to $\Delta\rho \equiv \rho - 1$ for the parameters corresponding to our examples.

To simplify the phenomenological analysis in the case of the unconstrained MSSM, we will assume the left– and right–handed stop mass parameters to be equal, $m_{\tilde{t}_L} = m_{\tilde{t}_R} \equiv m_{\tilde{q}}$. For illustration, we have chosen two somewhat extreme values for $\tan\beta$: $\tan\beta = 3$ and $\tan\beta = 30$. Large values of $\tan\beta$ maximize the h boson mass and therefore circumvent the present experimental lower bound on M_h in the decoupling limit, $M_h \gtrsim 90$ GeV [9], almost independently of the values of the parameter A_t chosen in our illustrations. For other values of the parameter $\tan\beta$, the $g_{h\tilde{t}_1\tilde{t}_1}$ coupling is simply obtained by rescaling the parameter $\tilde{A}_t = A_t - \mu/\tan\beta$. Note that for small values of $\tan\beta$, $\tan\beta \lesssim 3$, the CCB constraints are slightly less stronger than for larger values, while the constraint from the ρ parameter is almost independent of $\tan\beta$. An advantage of low $\tan\beta$ values is that, for the same value of $\tilde{A}_t$ and thus the $g_{h\tilde{t}_1\tilde{t}_1}$ coupling, M_h is smaller, allowing for more phase space and thus increasing the cross section, but eventually reaching its present lowest limit for a too small value of A_t.

In the case of the minimal SUGRA model [15], in which universality at the GUT scale implies that the only free parameters [1] are the values of m_0, $m_{1/2}$, A_0, respectively the common scalar mass, gaugino mass and trilinear scalar coupling, plus the sign of the μ parameter and $\tan\beta$. All the physical parameters, and in particular the squark masses, are obtained from a renormalization group (RG) running from the GUT scale to the weak scale [16], where the electroweak symmetry breaking constraints fix the $|\mu|$ and B parameters of the Higgs potential at the electroweak scale. [The RG evolution of the relevant parameters and calculation of the physical masses and couplings is done with the numerical code SUSPECT [22].] For the numerical illustrations, we choose specific values of the above parameters in such a way that one of the top squarks can be sufficiently light in order to have sizeable cross sections.

3. Associated production at e^+e^- colliders

At e^+e^- colliders, the final state $\tilde{q}_1\tilde{q}_1 h$ may be generated in three ways: (*i*) two–body production of a mixed pair of squarks and the decay of the heaviest squark to the lightest one and a Higgs boson [Fig. 1a]; (*ii*) the continuum production in e^+e^- annihilation [Fig. 1b]; and (*iii*) the continuum production in $\gamma\gamma$ collisions [Fig. 1c]. The same picture holds for the associated production of the heavier CP–even Higgs boson H with $\tilde{q}_1\tilde{q}_1$ pairs. In the case of the pseudoscalar boson A, only the processes (*i*) and (*ii*) are possible: because of CP–invariance, the coupling $A\tilde{q}_1\tilde{q}_1$ is absent and the final state $\tilde{q}_1\tilde{q}_1 A$ cannot be generated in $\gamma\gamma$ collisions at tree–level; furthermore, in e^+e^- annihilation the graph where the A boson is emitted from the Z line is absent, but there is another graph involving the $ZAh(H)$ coupling [see Fig. 1b]. For the associated production of CP–even Higgs bosons with $\tilde{q}_2\tilde{q}_2$ states, only the processes (*ii*) and (*iii*) are relevant.

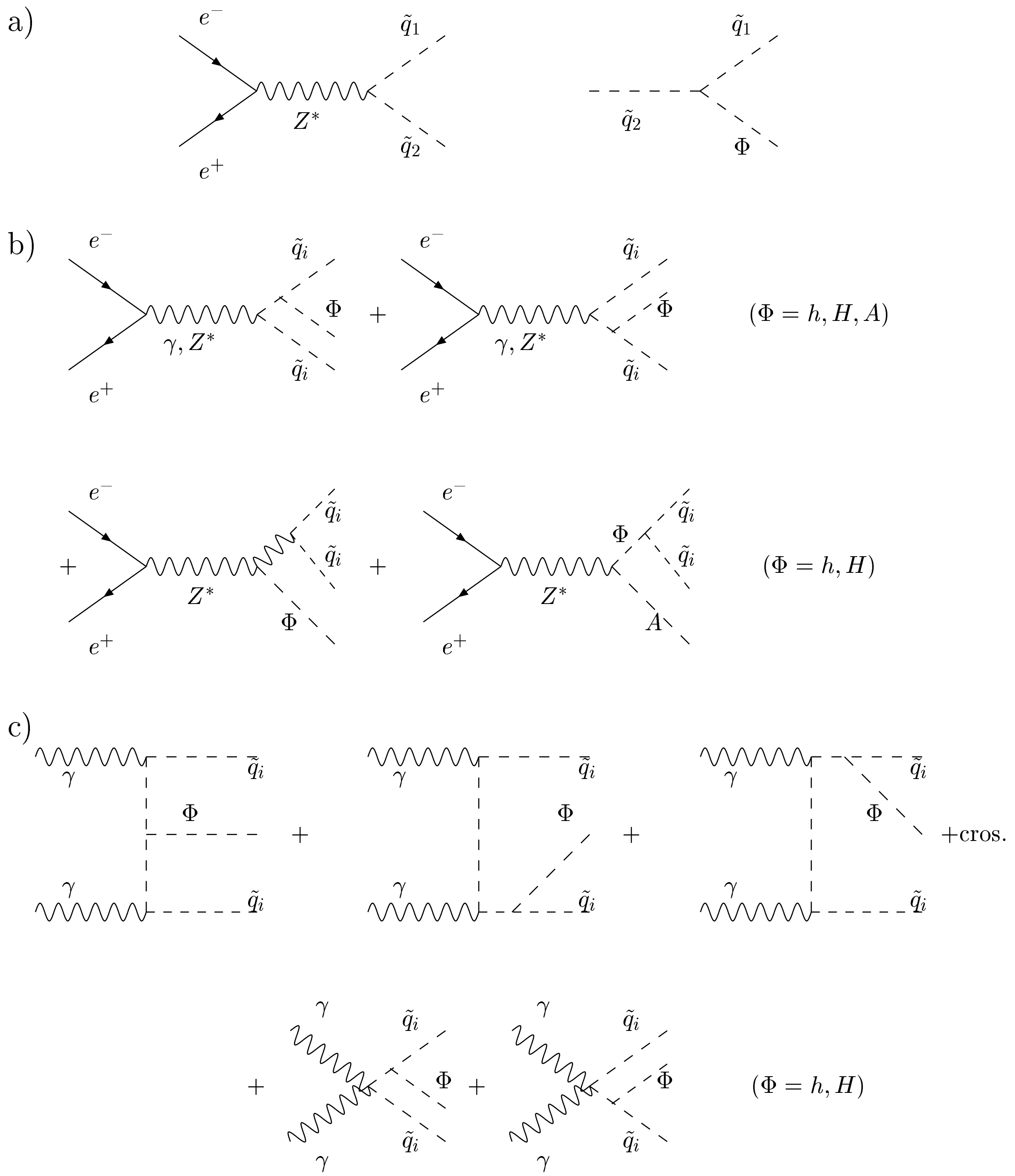

Figure 1: Feynman diagrams for the production of a Higgs boson Φ in association with a pair of squarks in e^+e^- and $\gamma\gamma$ collisions.

4.1 Two–body production and decay

If the center of mass energy of the e^+e^- collider is high enough, one can generate a $\tilde{q}_1\tilde{q}_1 h$ final state by first producing a mixed pair of squarks, $e^+e^- \to \tilde{q}_1\tilde{q}_2$, through the exchange of a virtual Z–boson, and then let the heaviest squark decay into the lightest one and the Higgs boson, $\tilde{q}_2 \to \tilde{q}_1 h$, if the splitting between the two squarks is larger than M_h; Fig. 1a. For H and A bosons final states, a larger splitting in the stop sector is required.

The total cross section [the QCD corrections to this process, including the SUSY–QCD contributions with the exchange of gluinos, are available [24] and can be included] is directly proportional to the coupling $g_{Z\tilde{q}_1\tilde{q}_2} \sim \sin 2\theta_q$ and in the case where the mixing between squarks is absent, this coupling is zero and the cross section vanishes.

The partial decay width of the heaviest squark into the lightest squark and a neutral Higgs boson [here also the QCD corrections are available [25] and can be included] is proportional to the $g_{\Phi\tilde{q}_1\tilde{q}_2}$ coupling. As can be seen from inspection of eq. (6), in contrast to the $g_{\Phi\tilde{q}_1\tilde{q}_1}$ coupling, $|g_{\Phi\tilde{q}_1\tilde{q}_2}|$ cannot be too large in most of the parameter space, and in fact this coupling is well dominated by its second term, proportional to $\cos 2\theta_q$, except for very large $\tilde{A}_t$ and/or when the mixing between squarks is maximal, $|\theta_q| = \pi/4$, in which case it is anyway practically vanishing.

The branching ratio for the $\tilde{q}_2 \to \tilde{q}_1\Phi$ decay mode is obtained by dividing the partial width by the total $\tilde{q}_2$ decay width. The latter is obtained by summing the widths of all possible decay channels. For instance, in the case of the more phase–space favored decay channel $\tilde{t}_2 \to \tilde{t}_1 h$, one has to include: decays of the $\tilde{t}_2$ into a bottom squark and a charged Higgs or W boson, decays into $\tilde{t}_1$ and a neutral Higgs or Z boson, decays into a b quark and charginos, and decays into a top quark and neutralinos [or gluinos].

In principle, if phase–space allowed, the cross section for the two–body production process times the branching ratio for the two–body decay, should be large enough for the final state to be copiously produced. However, as discussed above, in a large part of the parameter space the cross section times branching ratio will be roughly proportional to $\sin 2\theta_q \times \cos 2\theta_q$, thus giving small production rates in the no mixing and maximal mixing scenarii. In addition, the decay width $\tilde{q}_2 \to h\tilde{q}_1$ is in general much smaller than the $\tilde{q}_2$ decay widths into chargino and neutralinos, leading to a small branching ratio. Nevertheless, there are regions of the MSSM parameter space where the combination $\sin 2\theta_q \times \cos 2\theta_q$ can be maximal, which occurs typically for a not too small $m_{\tilde{t}_L}$–$m_{\tilde{t}_R}$ splitting and a moderate $\tilde{A}_t$. In this case [which is often realized in particular in the mSUGRA case, as we shall discuss next] the resonant $\tilde{t}_2$ process may dominate over the non-resonant $\tilde{t}_1\tilde{q}_1 h$ production and the corresponding rate is visible for the high luminosities $\int \mathcal{L}dt \sim 500$ fb^{-1} expected at linear colliders [26].

Such a situation is illustrated in the case of the $\tilde{t}_1\tilde{t}_1 h$ final state in Fig. 2, where the cross section $e^+e^- \to \tilde{t}_1\tilde{t}_2$ times the branching ratio BR($\tilde{t}_2 \to \tilde{t}_1 h$) is shown as a function of the $\tilde{t}_1$ mass at a c.m. energy of $\sqrt{s} = 800$ GeV [full lines]. We have chosen an mSUGRA scenario with $\tan\beta = 30$, $m_{1/2} = 100$ GeV, $A_0 = -600$ GeV and sign(μ) = +. [The broken lines show the contribution of the non–resonant contributions in this case, which will be discussed in more detail later]. As can be seen, the cross section can reach the level of 1 fb for relatively small $m_{\tilde{t}_1}$ values, leading to more than one thousand events in the course of a few years, with the expected luminosity of $\int \mathcal{L}dt \sim 500$ fb^{-1} [26].

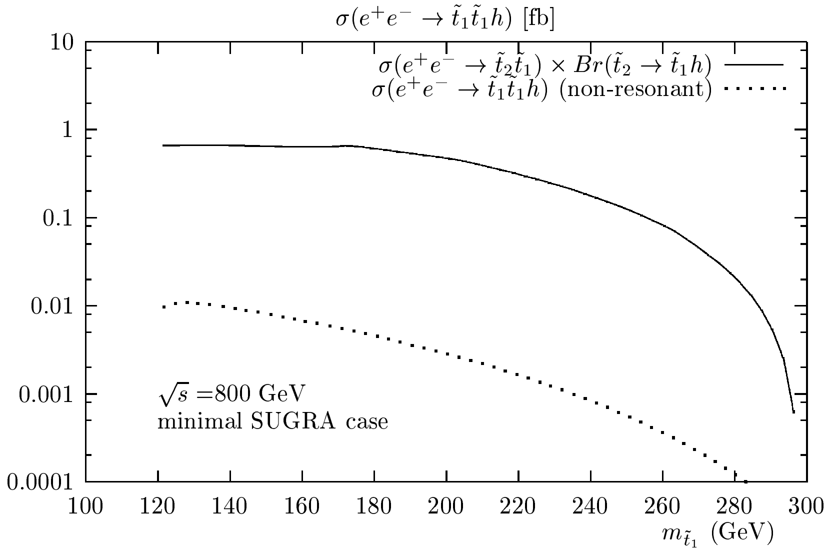

Figure 2: The production cross section $\sigma(e^+e^- \to \tilde{t}_1\tilde{t}_1 h)$ [in fb] as a function of $m_{\tilde{t}_1}$ in the mSUGRA case; $\tan\beta = 30$, $m_{1/2} = 100$ GeV and $A_0 = -600$ GeV.

Top squarks in this mass range will mainly decay into [23] a charm+neutralino, $\tilde{t}_1 \to c\chi_1^0$, or a b quark and a chargino, $\tilde{t}_1 \to b\chi^+$ [with the chargino being eventually off–shell]. In this latter case the lightest chargino, χ_1^+ will decay into the LSP and a real or virtual W boson, leading to the same topology as in the case of the top quark decay, but with a large amount of missing energy due to the undetected LSP. In e^+e^- collisions one can use the dominant decay mode of the lightest Higgs boson, $h \to b\bar{b}$. The final state topology will consist then of $4b$ quarks [two of them peaking at an invariant mass M_h, which would be already measured by means of another process], two [real or virtual] W's and missing energy. With the help of efficient micro–vertex detectors, this spectacular final state should be rather easy to detect in the clean environment of e^+e^- colliders.

4.2 Production in the continuum in e$^+$e$^-$ collisions

There are three types of Feynman diagrams leading to final states with $\tilde{q}_1\tilde{q}_1$ pairs and a CP–even Higgs boson h or H, in e^+e^- annihilation: Higgs boson emission from the $\tilde{q}_1$ states [which are produced through s–channel photon and Z–boson exchange], Higgs boson emission from the $\tilde{q}_2$ state [which is produced with $\tilde{q}_1$ through Z–boson exchange], and Higgs boson emission from a virtual Z boson which then splits into $\tilde{q}_1\tilde{q}_1$ pairs. When the Higgs–$\tilde{q}_1\tilde{q}_1$ couplings are large, the two last types of Feynman diagrams give negligible contributions since the virtuality of $\tilde{q}_2$ is large and the $Z\tilde{q}_1\tilde{q}_1$ coupling not enhanced. For the CP–odd Higgs boson the first and last possibilities are absent because of CP–invariance which forbids the couplings of A to gauge bosons and $\tilde{q}_1\tilde{q}_1$ pairs.

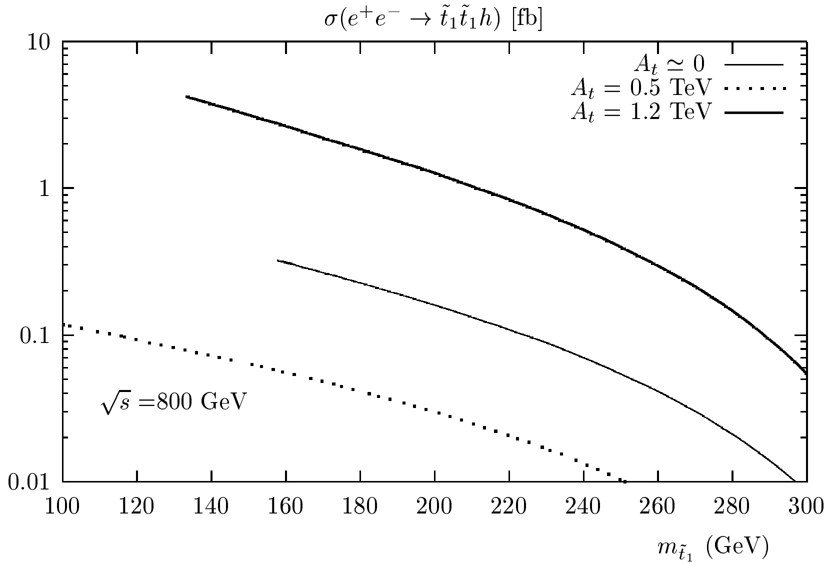

Figure 3: The cross section $\sigma(e^+e^- \to \tilde{t}_1\tilde{t}_1h)$ [in fb] as a function of $m_{\tilde{t}_1}$ and three different choices of the other parameters: $\tan\beta = 30$, $A_t = 0$ (0.5) TeV; $\tan\beta = 3$, $A_t = 1.2$ TeV.

To illustrate the magnitude of the cross sections, we show in Figs. 3–4 the rates for the $\tilde{t}_1\tilde{t}_1h$ final state in the decoupling limit at $\sqrt{s} = 800$ GeV and $\tan\beta = 30(\tan\beta = 3)$ as a function of the $\tilde{t}_1$ mass for $A_t \simeq 0$ and $A_t = 0.5$ TeV ($A_t = 1.2$ TeV) respectively [Fig. 3], and as a function of A_t for $m_{\tilde{t}_1} = 165$ GeV ($\tan\beta = 3$), and 250 GeV ($\tan\beta = 30$) [Fig. 4]. The cross section behaves as follows:

– In the case where there is no mixing in the stop sector, $\tilde{t}_1$ and $\tilde{t}_2$ have almost the same mass [which, up to the small contribution of the D–terms, is constrained to be larger than $m_t^{\overline{\rm MS}} \simeq 165$ GeV for $m_{\tilde{q}}^2 > 0$] and approximately the same couplings to the h boson since the m_t^2/M_Z^2 components in eq. (12) are dominant. The cross section in Fig. 3, which should then be multiplied by a factor of two to take into account the production of both top squarks, is smaller than the cross section for the SM–like process $e^+e^- \to t\bar{t}h$ [which is of the order of 2 fb for $M_h \sim 130$ GeV [14] at this c.m. energy] even in the low mass range, $m_{\tilde{t}} \lesssim 200$ GeV. [In scenarii where the $\tilde{t}$ masses are related to the masses of the light quark partners $m_{\tilde{q}}$, the mass range $m_{\tilde{t}} \lesssim 180$ GeV in the no mixing case is, however, ruled out by present experimental constraints on $m_{\tilde{q}}$ from the Tevatron [9].]

– For intermediate values of $\tilde{A}_t$ the two components of the $h\tilde{t}_1\tilde{t}_1$ coupling interfere destructively [with our conventions, $\sin 2\theta_t < 0$ in the relevant parameter space, see eq.(3)] partly canceling each other and resulting in a small cross section, unless $m_{\tilde{t}_1} \lesssim 100$ GeV. For some value of $\tilde{A}_t$, $g_{h\tilde{t}_1\tilde{t}_1} \sim 0$ and the cross section vanishes.

– In the large mixing case, $A_t \sim 1.2$ TeV, $\sigma(e^+e^- \to \tilde{t}_1\tilde{t}_1h)$ can be quite large without conflicting with the present bounds on M_h, the rho parameter or the CCB constraints. [The range of $\tilde{t}_1$ masses below $m_{\tilde{t}_1} \lesssim 130$ GeV where the cross section is the largest, gives too large contributions to the ρ parameter for this specific large value of $\tilde{A}_t$, and is also

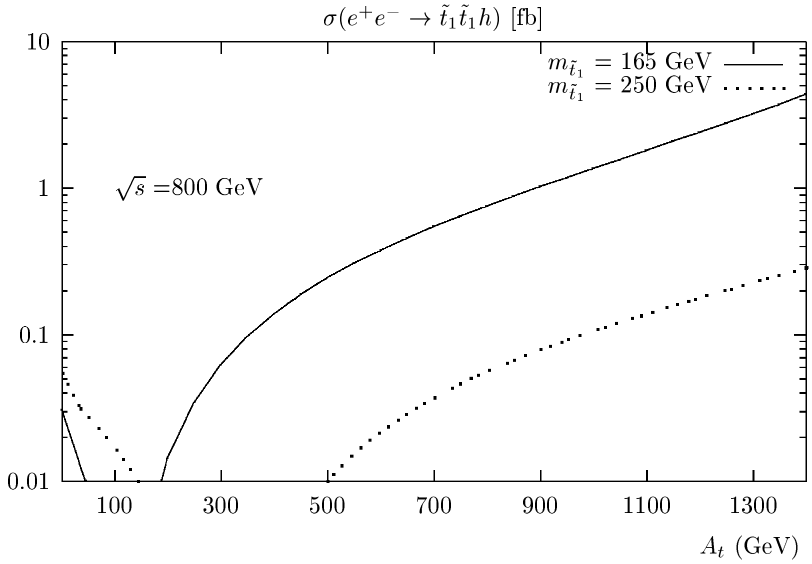

Figure 4: The cross section $\sigma(e^+e^- \to \tilde{t}_1\tilde{t}_1 h)$ [in fb] as a function of A_t for fixed $m_{\tilde{t}_1} = 165$ ($\tan\beta = 3$); and 250 GeV ($\tan\beta = 30$).

excluded already by the h boson mass lower bound.] If $\tilde{t}_1$ is lighter than the top quark, the $\tilde{t}_1\tilde{t}_1 h$ cross section significantly exceeds the one for $\bar{t}th$ final states.

At lower energies, the cross section can be as large as in the previous case for small $m_{\tilde{t}_1}$, but will be limited by phase space for larger values. This is illustrated in Fig. 5, with the same choice of parameters as in Fig. 3, but with a c.m. energy of $\sqrt{s} = 500$ GeV.

Thus, for not too large $m_{\tilde{t}_1}$ and large values of $\tilde{A}_t$, the production cross sections can exceed the value $\sigma(e^+e^- \to \tilde{t}_1\tilde{t}_1 h) \sim 1$ fb even at a c.m. energy of $\sqrt{s} = 500$ GeV. This provides more than one thousand events in a few years, with a luminosity $\int \mathcal{L}dt \sim 500$ fb^{-1}: a sample which should be sufficient to isolate the final state [with the topologies discussed previously] and measure the $g_{\tilde{t}_1\tilde{t}_1 h}$ coupling with some accuracy.

In the mSUGRA case the cross section can be as large as in the case of the unconstrained MSSM, but in a relatively smaller area of the SUSY parameter space. This is essentially due to the fact that it is generically very difficult to have almost degenerate $\tilde{t}_L$ and $\tilde{t}_R$ in mSUGRA as already discussed, so that the stop mixing angle which is controlled by the ratio $\tilde{A}_t/(\tilde{m}^2_{\tilde{t}_L} - \tilde{m}^2_{\tilde{t}_R})$ can become large only for very large $\tilde{A}_t$. Moreover in the RG evolution [16], $|A_t|$ tends to decrease when the energy scale is decreasing from GUT to low-energy. This makes a large A_t value at low energy less likely, since $A_0 = A_t(\mathrm{GUT})$ would have to be even larger, which may conflict with e.g. the CCB constraints. The only way to have an increasing $|A_t|$ when running down to low energy is if $A_0 < 0$ with A_0 small enough. This requires a large $m_{1/2}$ value, which implies not too small $m_{\tilde{t}_1}$.

Note finally that in the unconstrained MSSM case, the continuum production cross section in e^+e^- annihilation $\sigma(e^+e^- \to \tilde{t}_1\tilde{t}_1 h)$ is often larger than the resonant cross section for the production of $\tilde{t}_1\tilde{t}_2$ and the subsequent 2–body decay $\tilde{t}_2 \to \tilde{t}_1 h$, but this is not generic. Indeed, in a situation where both a non-negligible $m_{\tilde{t}_L}$–$m_{\tilde{t}_R}$ splitting and a

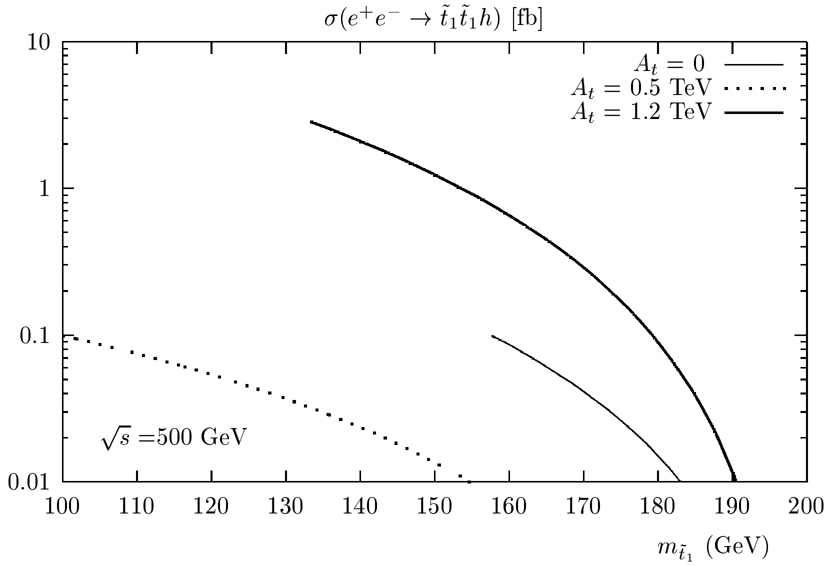

Figure 5: Same as Fig. 3 but with $\sqrt{s} = 500$ GeV.

moderate $\tilde{A}_t$ occurs, provided there is sufficient phase space, the production via a resonant $\tilde{t}_2$ becomes competitive, as previously illustrated in a typical mSUGRA casein Fig. 2.

4.3. Production in the continuum in $\gamma\gamma$ collisions

Future high–energy e^+e^- linear colliders can be turned into high–energy $\gamma\gamma$ colliders, with the high energy photons coming from Compton back–scattering of laser beams. The c.m. energy of the $\gamma\gamma$ collider is expected to be as much as $\sim 80\%$ of the one of the original e^+e^- machine. However, the total luminosity is expected to be somewhat smaller than the one of the e^+e^- mode, leading to a smaller number of events for the same cross section.

The final state $\tilde{q}_i\tilde{q}_i h$ or H can be generated by emitting the h, H bosons from the squark lines in the process $\gamma\gamma \to \tilde{q}_i\tilde{q}_i$; Fig. 1c. The pseudoscalar Higgs boson A cannot be produced in two–photon collisions in association with a pair of squarks because of CP–invariance; the production of the A boson is only possible in association with $\tilde{q}_1\tilde{q}_2$ states which is less favored by phase space.

The total cross section for the process $\gamma\gamma \to \tilde{t}_1\tilde{t}_1 h$ is shown in Fig. 6 at a two–photon c.m. energy $\sqrt{s}_{\gamma\gamma} \lesssim 0.8\sqrt{s}_{ee} = 600$ GeV and as a function of the $\tilde{t}_1$ mass, without convolution with the photon spectrum and with the same inputs and assumptions as in Fig. 3 to compare with the e^+e^- mode. Because the c.m. energy of the $\gamma\gamma$ collider is only $\sim 80\%$ of the one of the original e^+e^- machine, the process is of course less phase–space favored than in the e^+e^- mode. Nevertheless, the cross section for the $\tilde{t}_1\tilde{t}_1 h$ final state is of the same order as in the e^+e^- mode for c.m. energies not too close to the kinematical threshold, and the process might be useful to obtain complementary information since it does not involve the Z–boson and $\tilde{t}_2$ exchanges. If the luminosities of the $\gamma\gamma$ and e^+e^- colliders are comparable, a large number of events might be collected for small stop masses and large A_t values.

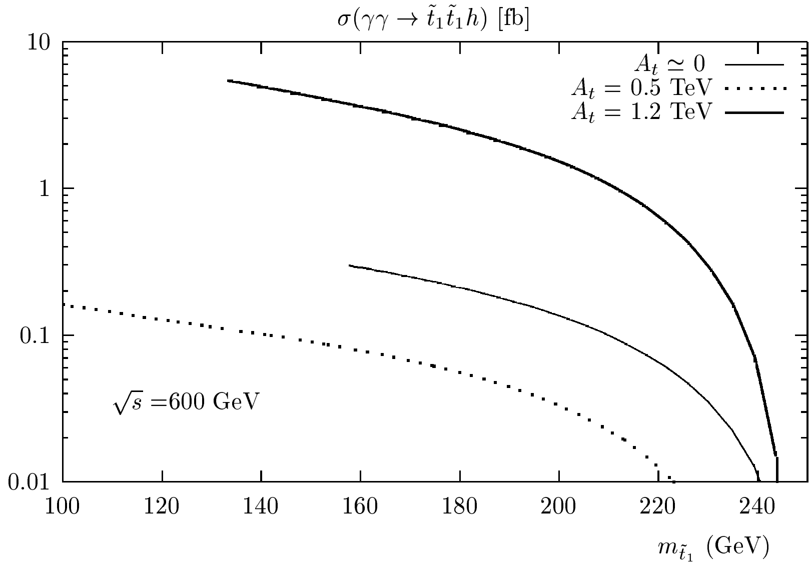

Figure 6: The cross section $\sigma(\gamma\gamma \to \tilde{t}_1\tilde{t}_1 h)$ in $\gamma\gamma$ collisions [in fb] at a c.m. energy $\sqrt{s_{\gamma\gamma}} = 600$ GeV as a function of $m_{\tilde{t}_1}$. The other parameters are as in Fig. 5.

5. Conclusions

We have analyzed the cross sections for the production of neutral Higgs particles of the MSSM in association with the supersymmetric scalar partners of the third generation quarks, $e^+e^- \to \tilde{q}_i\tilde{q}_i\Phi$, at e^+e^- colliders, in both the e^+e^- annihilation and the $\gamma\gamma$ fusion mode. In this numerical analysis, we focussed on the production of the lightest CP–even Higgs boson in the decoupling regime, in association with a pair of the lightest top squarks. Final states with the other Higgs bosons or with $\tilde{q}_1\tilde{q}_2$ pairs should be phase–space suppressed.

At e^+e^- colliders with c.m. energies around $\sqrt{s} = 800$ GeV and with very high luminosities $\int \mathcal{L}dt \sim 500$ fb^{-1}, the process $e^+e^- \to \tilde{t}_1\tilde{t}_1 h$ can lead to several hundreds of events, since the cross sections [in particular for rather light top squarks, $m_{\tilde{t}_1} \lesssim 250$ GeV and large trilinear coupling, $\tilde{A}_t \gtrsim 1$ TeV] can exceed the level of a 1 fb, and thus the rate for the standard–like process $e^+e^- \to t\bar{t}h$. In the case where the top squark decays into a b quark and a real/virtual chargino, the final state topology [with $4b$ quarks, missing energy and additional jets or leptons] will be rather spectacular and should be easy to be seen experimentally, thanks to the clean environment of these colliders. In the $\gamma\gamma$ option of the e^+e^- collider, the cross sections are similar as previously far from the particle thresholds, but are suppressed for larger masses because of the reduced c.m. energies. For $\gamma\gamma$ luminosities of the same order as the original e^+e^- luminosities, the $\tilde{t}_1\tilde{t}_1 h$ final state should also be observable in some areas of the parameter space.

The production cross section of the $\tilde{t}_1\tilde{t}_1 h$ final state is directly proportional to the square of the $\tilde{t}_1\tilde{t}_1 h$ couplings, the potentially largest electroweak coupling in the MSSM. Analyzing these final states at e^+e^- machines will allow to measure this coupling, opening thus a window to probe directly some of the soft–SUSY breaking scalar terms.

References

[1] For reviews on Supersymmetry and the MSSM see: H. P. Nilles, Phys. Rep. 117 (1985) 1; P. Nath, R. Arnowitt and A. Chamseddine, *Applied N=1 Supergravity*, ICTP series in Theoretical Physics, World Scientific, Singapore, 1984; Haber and G. Kane, Phys. Rep. 117 (1985) 75.

[2] For a review on the MSSM Higgs sector, see J.F. Gunion, H.E. Haber, G.L. Kane and S. Dawson, *The Higgs Hunter's Guide*, Addison–Wesley, Reading 1990.

[3] Y. Okada, M. Yamaguchi and T. Yanagida, Prog. Theor. Phys. 85 (1991) 1; H. Haber and R. Hempfling, Phys. Rev. Lett. 66 (1991) 1815; J. Ellis, G. Ridolfi and F. Zwirner, Phys. Lett. 257B (1991) 83; R. Barbieri, F. Caravaglios and M. Frigeni, Phys. Lett. 258B (1991) 167; M. Carena, M. Quiros and C.E.M. Wagner, Nucl. Phys. B461 (1996) 407; H. Haber, R. Hempfling and A. Hoang, Z. Phys. C75 (1997) 539; S. Heinemeyer, W. Hollik and G. Weiglein, Phys. Lett. B440 (1998) 296.

[4] ATLAS Collaboration, Technical Proposal, Report CERN–LHCC 94–43; CMS Collaboration, Technical Proposal, Report CERN–LHCC 94–38.

[5] E. Accomando *et al.*, LC CDR Report DESY 97-100, Phys. Rep. 299 (1998) 1; A. Djouadi et al., Report DESY 96–123D, hep-ph/9605437; S. Kuhlman *et al.*, NLC ZDR Design Group and the NLC Physics Working Group, report SLAC–R–0485; A. Djouadi, hep-ph/9910449.

[6] M. Carena, P.M. Zerwas *et al.*, "Higgs Physics at LEP2", CERN Yellow Report CERN-96-01, hep–ph/9602250.

[7] Report of the Tev2000 study group on "Future Electroweak Physics at the Tevatron", D. Amidei and R. Brock, eds. (1995).

[8] J. Ellis and S. Rudaz, Phys. Lett. B128 (1983) 248; M. Drees and K. Hikasa, Phys. Lett. B252 (1990) 127.

[9] Particle Data Group, Eur. Phys. J. C3(1998) 1; for a slightly more recent collection of limits, see e.g. A. Djouadi, S. Rosier–Lees *et al.*, hep–ph/9901246.

[10] CDF collaboration, contribution ICHEP98, Vancouver, FERMILAB-Conf-98/208-E.

[11] A. Djouadi, Phys. Lett. B435 (1998) 101; A. Djouadi *et al.*, Eur. Phys. J. C1 (1998) 149; A. Djouadi, J.L. Kneur and G. Moultaka, Phys. Rev. Lett. 80 (1998) 1830; G. Bélanger *et al.*, hep–ph/9811334; A. Dedes and S. Moretti, hep–ph/9812328 and hep-ph/9904491; G. Bélanger *et al.*, hep-ph/0002258.

[12] G. Bélanger, F. Boudjema, T. Kon and V. Lafage, hep-ph/9904348.

[13] A. Djouadi, J.L. Kneur and G. Moultaka, hep-ph/9903218.

[14] A. Djouadi, J. Kalinowski and P. Zerwas, Z. Phys. C54 (1992) 255 and Mod. Phys. Lett. A7 (1992) 1765; S. Dittmaier *et al.*, Phys. Lett. B441 (1998) 383; S. Dawson and L. Reina, Phys. Rev. D57 (1998) 5851; S. Moretti, hep–ph/9902214.

[15] A.H Chamseddine, R. Arnowitt and P. Nath, Phys. Rev. Lett. 49 (1982) 970; R. Barbieri, S. Ferrara and C.A Savoy, Phys. Lett. B119 (1982) 343; L. Hall, J. Lykken and S. Weinberg, Phys. Rev. D27 (1983) 2359.

[16] See for instance, D.J. Castaño, E.J. Piard and P. Ramond, Phys. Rev. D49 (1994) 4882; W. de Boer, R. Ehret and D.I. Kazakov, Z. Phys. C67 (1994) 647; V. Barger, M.S. Berger and P. Ohmann, Phys. Rev. D49 (1994) 4908.

[17] M. Carena *et al.*, Nucl. Phys. B426 (1994) 269; W. de Boer, R. Ehret and D.I. Kazakov, Z. Phys. C67 (1994) 647; See also M. Drees and S. Martin, hep–ph/9504324.

[18] See for instance H.E. Haber, CERN-TH/95-109 and hep–ph/9505240.

[19] J.F. Gunion A. Stange and S. Willenbrock, hep–ph/9602238.

[20] For a recent review, see: J.A. Casas, A. Lleyda and C. Muñoz, Nucl. Phys. B471(1996) 3.

[21] See for instance, J. Erler and P. Langacker, hep–ph/9809352; G.C. Cho *et al.*, hep–ph/9901351, A. Djouadi, hep-ph/9911468.

[22] A. Djouadi, J.-L. Kneur and G. Moultaka, SUSPECT: a program for the MSSM spectrum, in hep-ph/9901246.

[23] K.I. Hikasa and M. Kobayashi, Phys. Rev. D36 (1997) 724; C. Boehm, A. Djouadi and Y. Mambrini, hep-ph/9907428.

[24] A. Arhrib, M. Capdequi-Peyranere and A. Djouadi, Phys. Rev. D52 (1995) 1404; H. Eberl, A. Bartl and W. Majerotto, Nucl. Phys. B472 (1996) 481.

[25] A. Arhrib *et al.*, Phys. Rev. D57 (1998) 5860; A. Bartl *et al.*, hep–ph/9806299.

[26] See the Working Group "Machine-Experiment Interface", 2nd Joint ECFA/DESY Study on Linear Colliders, Orsay–Lund–Frascati–Oxford, 1998–1999 at the web site: http://www.desy.de/ njwalker/ecfa-desy-wg4/index.html .

[27] I.F. Ginzburg *et al.*, Nucl. Instrum. Meth. 205 (1983) 47 and 219 (1984) 5; V.I. Telnov, Nucl. Instrum. Meth. A294 (1990) 72 and A335 (1995) 3.